

Diamond and SiC Semi-Confocal Acoustic Resonator

CNF Project Number: 2126-12

Principal Investigator(s): Gregory D. Fuchs¹

User(s): Huiyao Chen²

Affiliation(s): 1. School of Applied and Engineering Physics, 2. Department of Physics; Cornell University

Primary Source(s) of Research Funding: Office of Naval Research (Grants No. N000141410812 and No. N000141712290)

Contact: gdf9@cornell.edu, hc846@cornell.edu

Website: <http://fuchs.research.engineering.cornell.edu>

Primary CNF Tools Used: PT770 etcher, GCA 5x stepper, Heidelberg mask writer DWL2000, AJA sputtering deposition system, odd/even evaporator, YES Asher, P10 profilometer, Westbond 7400A ultrasonic wire bonder

Abstract:

We report the design and fabrication of a semi-confocal high-overtone bulk acoustic resonator (SCHBAR) device on diamond (silicon carbide) with $f \cdot Q > 10^{12}$ ($> 10^{13}$) [1]. The semi-confocal geometry confines the phonon mode laterally below 10 μm . The device also has integrated atomic-scale quantum defects, and is thus suitable for quantum control applications such as mechanical manipulation of the defect spin states.

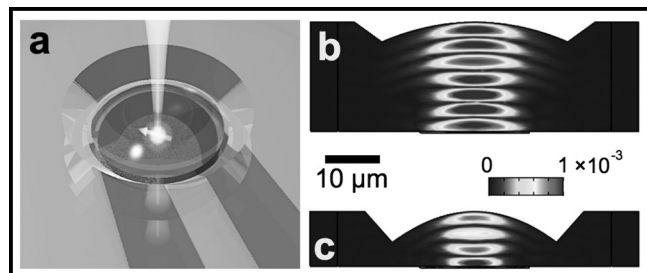


Figure 1: (a) Concept image of the semi-confocal HBAR device design. (b) and (c) are strain profiles of the diamond devices simulated by COMSOL for a 3 GHz mode, with a 1 V_p voltage driving source.

Summary of Research:

As illustrated in Figure 1, the device has a planar-convex structure. We design one side of the resonator with a curved surface, enabling it to confine three dimensional phonon modes with characteristic dimensions of 10 μm . The radius of curvature of the curved surface is twice the thickness of the substrate in a semi-confocal geometry, giving rise to the device name, SCHBAR.

Compared to a planar cavity, the curved surface eliminates the requirement of boundary parallelism and, in principle, yields higher mechanical quality factors. Optically, the curved surface also acts as a solid immersion lens (SIL) [2]. It reduces substrate refraction and thus enhances light extraction from the defects inside the resonator. The defects are microns below the surface and thus are well-protected from fabrication damage and surface effects. On the planar side of the device, we fabricate an integrated piezoelectric transducer and a microwave antenna that

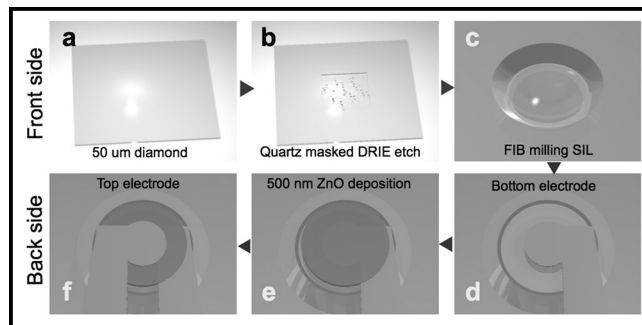


Figure 2: Fabrication process flow of the device starting from (a) a 50- μm -thick double-side-polished diamond plate; (b) DRIE etch a diamond membrane down to 20 μm or 10 μm using Ar/Cl_2 and O_2 plasma, using a laser cut quartz mask; (c) Mill the parabolic SIL using focused Ga ion beam. (d-f) A ZnO piezoelectric transducer is fabricated on the backside of the SIL.

is aligned with the center of the resonator, allowing for acoustic and magnetic driving, respectively. The radius of the transducer has been designed to mode-match the waist of the confined acoustic wave, and the thickness of piezoelectric ZnO film is controlled to target a 3 GHz resonance mode, which allows stable confinement.

We fabricated SCHBAR devices from both diamond and 4H-SiC substrates. For simplicity, we restricted the process flow description to diamond (Figure 2). We start from a 50- μm -thick, double-side polished single crystal diamond plate (nitrogen concentration < 1 ppm). In the first step, we etch 5 μm of diamond on each side of the substrate using Ar/Cl_2 [3] and O_2 [4] plasma as a stress-relief etch to eliminate the residual polishing damage. A laser-cut quartz shadow mask is then used to mask the

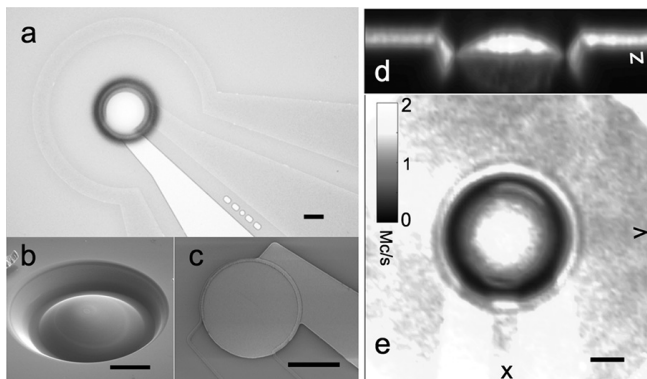


Figure 3: Micrographs and photoluminescence images of the finished device on an optical grade diamond substrate. (a) Device viewed from SIL side. (b) SEM of the milled solid immersion lens (radius of curvature 20 μm). (c) SEM of the transducer on the backside of the SIL. (d) and (e) show the photoluminescence image in a cross section view and a front view of the device (10 μm thick), collected using a home-built confocal microscope. The scale bars in all figures are 10 μm in length.

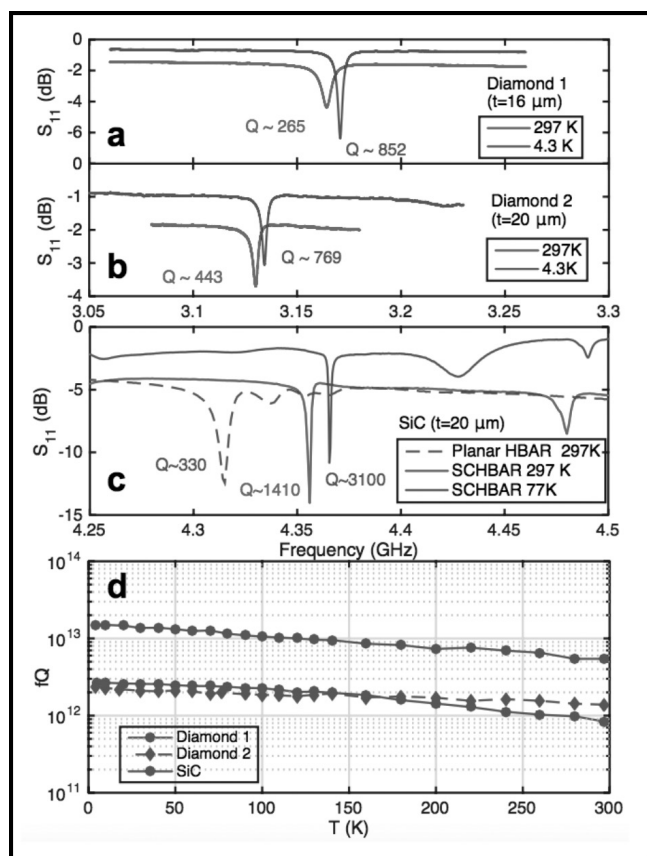


Figure 4: (a-c) S -parameters characterization of the device using a vector network analyzer. (d) Quality factors are extracted from the measured S -parameters as a function of temperature.

diamond for another 20- or 30- μm -deep etch on one side of the sample (etch rate 5 $\mu\text{m}/\text{hr}$). After lifting the quartz mask, we end up with a 10 μm or 20 μm diamond membrane suspended in a 40 μm frame. Atomic force microscopy (AFM) shows a surface roughness of < 0.3 nm.

A focused gallium ion beam (FIB, 30 kV, 20 nA) is used to mill the parabolic SIL structure on the diamond membrane. After FIB milling, the diamond surface is substantially graphitized and contains implanted gallium atoms (20 nm in depth). We then etch away the top 100 nm of damaged diamond using Ar/Cl_2 plasma, followed by a 120 nm O_2 plasma etch to oxygen terminate the diamond surface. A boiling tri-acid bath containing equal parts of sulfuric, nitric and perchloric acid is used to further clean off any residual contamination on the diamond. Optical profilometry and laser-scanning confocal microscopy have been used to confirm the profile accuracy of the SIL. The diamond membrane is then flipped with the planar side facing up. A piezoelectric zinc oxide (ZnO) transducer, consisting of bottom electrode (10 nm/90 nm Ti/Pt), 500 nm ZnO, top electrode (10 nm/180 nm Ti/Pt), and a microwave antenna are then lithographically defined and sputtered to finish the device fabrication.

We use a vector network analyzer (VNA) to characterize the scattering parameter (S -parameter) of the device. The mechanical quality factor of the device, Q , can be extracted from the VNA measurements. After mounting the devices in vacuum on a cold finger of a helium-flow cryostat, we perform electrical measurements as a function of temperature. The results are shown in Figure 4. The frequency and quality factor product is $f \cdot Q > 10^{12}$ for a 20- μm -thick diamond device at room temperature and $f \cdot Q > 10^{13}$ for a 20- μm -thick SiC device under cryogenic condition.

References:

- [1] Chen, H; Opondo, N. F; Jiang, B; MacQuarrie, E. R.; Daveau R. S.; Bhawe, S. A.; Fuchs G. D., arXiv: arXiv:1906.06309, 2019.
- [2] Hadden, J.; Harrison, J.; Stanley-Clarke, A.; Marseglia, L.; Ho, Y.-L.; Patton, B.; O'Brien, J.; Rarity, J. Applied Physics Letters 2010, 97, 241901.
- [3] Lee, C.; Gu, E.; Dawson, M.; Friel, I.; Scarsbrook, G. Diamond and Related Materials 2008, 17, 1292-1296.
- [4] Friel, I.; Clewes, S.; Dhillon, H.; Perkins, N.; Twitchen, D.; Scarsbrook, G. Diamond and Related Materials 2009, 18, 808-815.